Chemical Communications **2024**, *60*, 26, 3515-3518

https://pubs.rsc.org/en/content/articlelanding/2024/cc/d3cc06227a/

COMMUNICATION

Switching On Emission in Zn(II) Coordination Complexes by Tempering N_{amido} Character†

Received 00th January 20xx,
Accepted 00th January 20xx

DOI: 10.1039/x0xx00000x

Amy L. Knodel,[a] Issiah B. Lozada,[a] Robert J. Ortiz,[a] J. A. Gareth Williams[b]* and David E. Herbert[a]*

A series of four-coordinate zinc(II) complexes is presented in which the amido vs imino character of a ligated nitrogen donor correlates to the luminescence intensity. DFT analysis points to a distinct mechanism for this trend wherein emission can be switched on by restricting non-radiative decay pathways through the resonance-induced delocalization of amido ligand lone-pairs.

In the pursuit of sustainable and cost-effective light-emitting materials, zinc coordination complexes are an attractive target.[1] With competitive abundance to copper in the earth's crust and fewer competing industrial pressures,[2] Zn(II) also boasts a filled *d* subshell, limiting the involvement of parasitic metal-centered excited states that can depopulate those that are desirable for emission. Accordingly, luminescence from Zn(II) complexes tends to be dominated by excited states with ligand-centred (e.g., intraligand charge transfer or ILCT) character and thus can be highly sensitive to ligand structure.[3] A number of mechanisms have been identified that influence emission, including the integration of luminophores in supramolecular frameworks,[4,5] aggregation effects,[6] thermally activated delayed fluorescence,[7,8] and the participation of symmetry-breaking charge-transfer (SBCT) excited states.[9,10] Outside of zinc porphyrins, pseudo-tetrahedral Zn(II) species supported by a pair of monoanionic, N^O-type bidentate ligands typify many luminescent examples that emit from discrete, monomeric excited states in fluid solution.[11] One feature, however, that appears to be generally detrimental to efficient emission in this context is the presence of a Zn–N_{amido} unit. For example, homoleptic Zn complexes of azadipyrromethene ligands[12] (Figure 1a) are non-emissive, despite the intense luminescence displayed by their BF_2 congeners[13] and isoelectronic coinage metal analogs.[14] Zn–N_{imino} motifs, on the other hand, can be conducive to quite bright luminescence in homoleptic complexes (Figure 1b).[15]

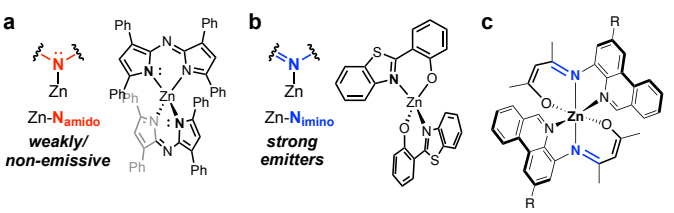

Figure 1. (a) Zn–N_{amido} as in non-emissive *bis*(azadipyrromethene)zinc,[14] and (b) Zn–N_{imino} motifs, including selected examples of strongly emissive complexes such as *bis*(2-(2-hydroxyphenyl)benzothiazolato)zinc[16] and (c) yellow-emitting Zn(II) N^N^O complexes.[17]

Indeed, in our own work on homoleptic, pseudo-octahedral Zn(II) complexes that display intense yellow triplet-state emission,[17] we found that, despite being prepared via deprotonation of acidic NH bonds in keto-iminate '*nacac*'-style proligands, the ground state of these complexes is best described as having enolato-imine character in the ligand scaffold; that is, N_{imino} rather than N_{amido} character (Figure 1c). This suggested to us that tempering N_{amido} character might be used to turn on luminescence in otherwise non-emissive Zn coordination complexes. Here, we demonstrate this working principle through a series of four-coordinate Zn(II) complexes with N^N ligands of varying N_{amido} character. We show how luminescence can be switched on using ligand frameworks whose Lewis structures predict amido character but allow for delocalization of the nitrogen lone pair through resonance.

To test our hypothesis, we chose a series of ligands that – once appended to Zn(II) – would present varying degrees of $N_{amido/imino}$ character, while otherwise keeping as much as possible about the complexes the same (Figure 2). For example,

[a] *Department of Chemistry and the Manitoba Institute for Materials, University of Manitoba, 144 Dysart Road, Winnipeg, Manitoba, R3T 2N2, Canada; *david.herbert@umanitoba.ca.*

[b] *Department of Chemistry, Durham University, Durham, DH1 3LE, UK; *j.a.g.williams@durham.ac.uk.*

Electronic Supplementary Information (ESI) available: full experimental details, crystallographic information files (CIFs; CCDC 2320600-2320601) and supporting figures and tables. See DOI: 10.1039/x0xx00000x

†This work was supported by the Natural Sciences Engineering Research Council of Canada (RGPIN-2022-04501) and Compute Canada. Noah Martens is thanked for assistance with the crystal growth and structures of (^{CF3}**L1**)$ZnCl_2$ and (^{CF3}**L2**)$_2$Zn.

each ligand contains a phenanthridine (benzo[*c*]quinoline) heterocycle,[18] which can serve as an effective electron acceptor in charge-transfer excitations and provide a second *N*-donor to complete the chelate. ^{R}**L1** (R = *t*Bu or CF_3) contain a guanidine unit and bind as neutral L_2-type donors; they were used to prepare heteroleptic (^{R}**L1**)$ZnCl_2$ type complexes via reaction with zinc dichloride. ^{CF3}**L2** bears a 2-substituted pyrimidine; it retains the $(N)_2C$-N architecture of the guanidinyl unit but acts as an LX-type donor when deprotonated and bound to Zn in (^{CF3}**L2**)$_2$Zn, formed via reaction of two equivalents of the proligand with diethylzinc. In ^{tBu}**L3**, the pyrimidine is replaced by a phenyl ring, and again binds to Zn(II) as an LX-donor via a neutral phenanthridine and *N*-phenyl N_{amido}.[19] The identity of the substituent at the 2-position of the phenanthridinyl donor (*t*Bu or CF_3) does impact slightly the photophysics of pseudo-octahedral Fe(II) chromophores[20] and square-planar Pt(II) emitters[21] containing these units but, as will be seen below when comparing the two (^{R}**L1**)$ZnCl_2$ complexes, not to an extent here that influences the overall conclusions of this work.

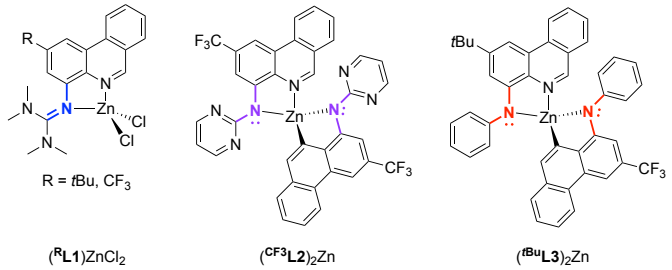

(^{R}**L1**)$ZnCl_2$ (^{CF3}**L2**)$_2$Zn (^{tBu}**L3**)$_2$Zn

Figure 2. The $LZnCl_2$ and L_2Zn complexes studied in this work.

Multinuclear NMR spectroscopy in solution is consistent with the formation of neutral, mononuclear complexes of each ligand. The distorted pseudo-tetrahedral geometries were also confirmed in the solid-state using single-crystal X-ray crystallography for (^{CF3}**L1**)$ZnCl_2$ and (^{CF3}**L2**)$_2$Zn (Figure 3a); the solid-state structure of (^{tBu}**L3**)$_2$Zn has been previously disclosed.[19] It is immediately evident that the C–N bond lengths connecting the ligating $N_{imino/amido}$ (N2) with either the guanidinyl $C(NMe_2)_2$ moiety in (^{CF3}**L1**)$ZnCl_2$ or the 2-pyrimidinyl fragment in (^{CF3}**L2**)$_2$Zn are similar and statistically shorter {N2-C15: 1.340(3) Å and 1.360(5) Å for those two complexes, respectively}} than in (^{tBu}**L3**)$_2$Zn {1.419(3)/1.410(3) Å}. This is consistent with C=N_{imino} double-bond character in the former two complexes and C–N_{amido} single-bond character in the latter. Clearly, then, the resonance contributor shown in Figure 3b for (^{CF3}**L2**)$_2$Zn influences the ground-state structure in the solid-state. Indeed, the planes formed by the phenanthridinyl ring system and the pyrimidinyl ring in (^{CF3}**L2**)$_2$Zn are nearly co-planar (dihedral angle = 8°), compared to an angle of 59° in (^{tBu}**L3**)$_2$Zn (Figure S9). Interestingly, the bond angles around the coordinating, acyclic nitrogen donors are somewhat counterintuitive. For an sp^2-hybridized nitrogen donor of predominantly N_{imino} character (e.g., N2 in (^{CF3}**L1**)$ZnCl_2$), a planar geometry might be expected, while an sp^3-hybridized N_{amido} (e.g., N2 in (^{tBu}**L3**)$_2$Zn) should conceivably exhibit pyramidalization at nitrogen. Instead, a nearly perfectly planar arrangement is observed about N2 in both (^{CF3}**L2**)$_2$Zn and (^{tBu}**L3**)$_2$Zn (sum of bond angles about N2 = 360°) with a more pyramidal arrangement in (^{CF3}**L1**)$ZnCl_2$ (sum of bond angles about N2 = 351.5°). Thus, in contrast to the bond distances, the similarities in bond angles about the coordinating $N_{imino/amido}$ atom are most pronounced between (^{CF3}**L2**)$_2$Zn and (^{tBu}**L3**)$_2$Zn.

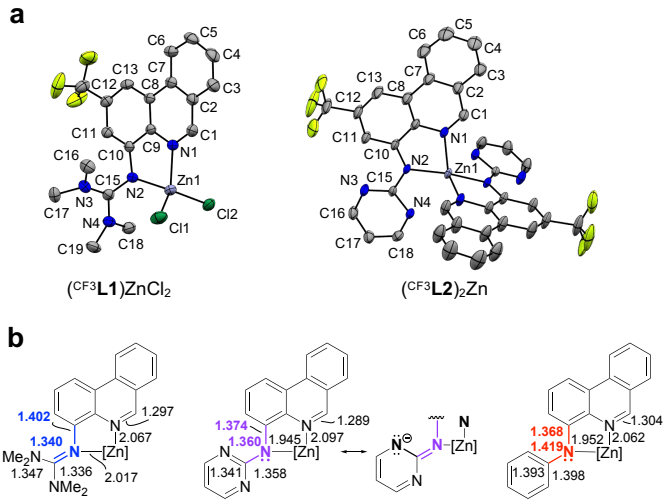

Figure 3. (a) Solid-state structures of (^{CF3}**L1**)$ZnCl_2$ and (^{CF3}**L2**)$_2$Zn with thermal ellipsoids shown at 50% probability levels. Hydrogen atoms, co-crystallized solvent molecules and selected atom labels omitted for clarity. (b) Selected bond lengths of (^{CF3}**L1**)$ZnCl_2$, (^{CF3}**L2**)$_2$Zn and (^{tBu}**L3**)$_2$Zn[19] (one of two sets of crystallographically distinct values) with an important resonance contributor shown for (^{CF3}**L2**)$_2$Zn, highlighting the N_{imino} character.

Gas-phase natural bond orbital (NBO) analysis supports the trend in N_{amido} vs N_{imino} character seen in the solid-state. NBO analysis was performed using eight different functionals to probe the effect of Hartree-Fock (HF) exchange on covalency and delocalization. For context, we also included emissive Zn(II)-N_{imino} N^N^O complexes[22] (^{R}**L4**)$_2$Zn (R = CF_3, *t*Bu, Me; Figure 1c) and a second non-emissive Zn(II)-N_{amido} *N*-phenyl complex[19] (^{Me}**L3**^{Me})$_2$Zn identical to (^{tBu}**L3**)$_2$Zn but with a Me group in place of the *t*Bu and a second Me at the 6-position adjacent to the phenanthridinyl nitrogen. For both (^{tBu}**L3**)$_2$Zn and (^{Me}**L3**^{Me})$_2$Zn, NBO confirms unequivocal N_{amido} character with two lone pairs identified at the coordinating acyclic nitrogen atoms. In comparison, NBO analysis of both (^{R}**L1**)$ZnCl_2$ complexes shows a single lone pair at the acyclic nitrogen donor and two bonding pairs to the guanidinyl carbon (i.e., N=$C(NMe_2)_2$). A similar situation is identified for the N^N^O *bis*-chelated (^{R}**L4**)Zn_2 series, in which solid-state crystallographic and IR spectroscopic data both point to N_{imino} character owing to a dominant imino-enolate resonance contributor.[22] For (^{CF3}**L2**)$_2$Zn, NBO analysis at higher levels of HF exchange (> 25%) is consistent with the N_{amido} Lewis structure, while at lower levels of HF exchange (< 25%), an N_{imino} structure is predicted (Figure 3b). The inclusion of implicit solvation (SMD[23]; CH_2Cl_2) yields the same results. Thus, NBO analyses, both in gas- and solution-phase, corroborate the presence of a significant N_{imino} resonance contributor for (^{CF3}**L2**)$_2$Zn, attributed to delocalization of the coordinating nitrogen's lone pair into the pyrimidine ring.

With the $N_{imido/amido}$ character of the molecular coordination complexes established, we turned to their electronic absorption

and emission spectra. The two heteroleptic (^{R}**L1**)ZnCl$_2$ complexes absorb light in a very similar manner to their uncomplexed proligands (Figure S3a). The two homoleptic complexes, (^{CF3}**L2**)$_2$Zn and (^{tBu}**L3**)$_2$Zn, display significantly red-shifted absorption maxima compared to ^{CF3}**L2** and ^{tBu}**L3**, with a much larger extinction. TD-DFT simulations of the (^{R}**L1**)ZnCl$_2$ complexes attribute the lowest energy absorption to transitions with intraligand charge transfer (ILCT) character, while the lowest-energy absorptions in the homoleptic (^{CF3}**L2**)$_2$Zn and (^{tBu}**L3**)$_2$Zn embody locally excited character. Upon excitation into the lowest energy absorption bands, the heteroleptic species (^{R}**L1**)ZnCl$_2$ display intense luminescence in solution (Figure 4a), with emission maxima of 512 nm and 530 nm and photoluminescence quantum yields (PLQY) of 0.64 and 0.41 respectively (Table 1). The emission is consistent with a spin-allowed fluorescence process, with lifetimes of around 12-13 ns that are unaffected by oxygen. At 77 K, the emission shifts slightly to higher energy. The two complexes remain emissive in the solid state, although the quantum yields are somewhat suppressed (0.22 and 0.045, respectively), probably through intermolecular quenching processes. The homoleptic Zn-amido species (^{tBu}**L3**)$_2$Zn is non-emissive in fluid solution, as reported previously.[19] Remarkably, we find here that the structurally analogous species (^{CF3}**L2**)$_2$Zn is luminescent with an emission maxima of 595 nm, shifted into the yellow region compared to the blue-emitting (^{R}**L1**)ZnCl$_2$ (Figure 4b vs 4a). The measured PLQYs (0.26 and 0.074 in solution and solid-state, respectively) and lifetime (8 ns in solution) are consistent with a similar photophysical process as in (^{R}**L1**)ZnCl$_2$ (for comparison with selected other Zn(II) luminophores, see Table S1).

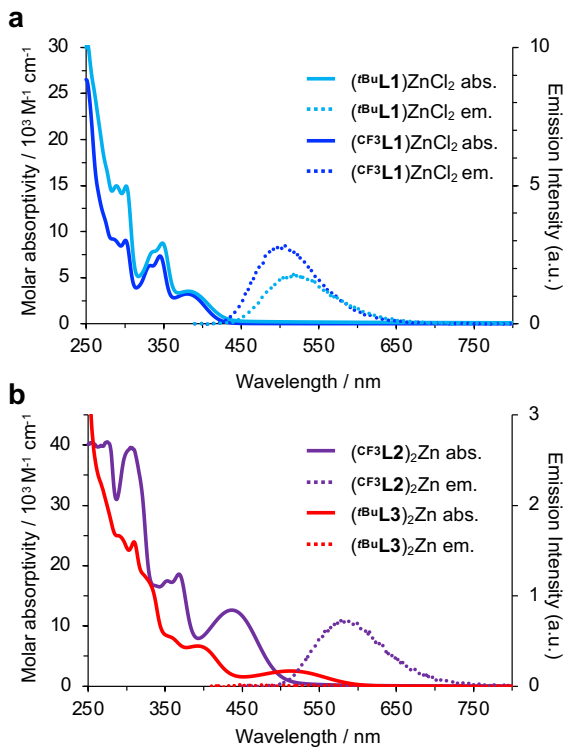

Figure 4. (a) Molar absorptivity and (b) unnormalized emission plots for equimolar solutions (1.0 x 10^{-4} M) in deoxygenated CH_2Cl_2 solution at 295 K. Excitation wavelengths were 380 nm for (^{R}**L1**)ZnCl$_2$, 440 nm (^{CF3}**L2**)$_2$Zn, and 400 nm (^{tBu}**L3**)$_2$Zn.

The unexpected, striking difference in the behaviour of (^{CF3}**L2**)$_2$Zn and (^{tBu}**L3**)$_2$Zn demanded further study. Homoleptic Zn(II) dipyrrins and related systems have been shown to form excited states characterized by a loss of electronic symmetry – i.e., symmetry-breaking charge transfer (SBCT) states – that effectively quench emission.[9,10] In such systems, less polar solvents favour the population of excited states with more localized character capable of radiative decay to the ground state.[24] To probe the participation of SBCT here, equimolar solutions of (^{CF3}**L2**)$_2$Zn and (^{tBu}**L3**)$_2$Zn were prepared in dichloromethane, diethyl ether, toluene and hexanes. A small degree of bathochromic solvatochromism is observed in the steady-state absorption spectra (Figure S4). However, contrary to literature examples of SBCT in four-coordinate Zn(II), emission intensity of (^{CF3}**L2**)$_2$Zn was seen to *decrease* with decreasing solvent polarity, while no evidence of luminescence was observed in any medium for (^{tBu}**L3**)$_2$Zn. TD-DFT analysis of both complexes in all four solvents shows that at the Frank-Condon geometry, two nearly isoenergetic excited states (S_1, S_2) initially form with the hole on the $N_{imino/amido}$/pyrimidinyl fragment {for (^{CF3}**L2**)$_2$Zn)} or N_{amido}/phenyl fragment {for (^{tBu}**L3**)$_2$Zn)} and the electron on the phenanthridinyl donor arm (Figures S17 and S20). At the optimized S_1 geometry, the two lowest-lying excited states separate in energy ($\Delta E_{S2\text{-}S1}$ ~ 0.4 eV) with intraligand charge transfer (ILCT) character assigned to the lower energy S_1 and interligand SBCT character to the higher energy S_2. This relative energetic ordering is maintained for both complexes in all solvents, and thus the observed 'turn-on' of emission cannot be attributed to SBCT.

For both (^{CF3}**L2**)$_2$Zn and (^{tBu}**L3**)$_2$Zn, decreasing solvent polarity does narrow the energy gap between the S_2 state at the ground-state geometry and the S_2 state at the S_1-optimized geometry, which could contribute to emission quenching in lower-polarity solvents. Similarly, the energy difference between the lowest-lying triplet excited state (T_1) and the S_1 state also decreases with decreasing solvent polarity at all geometries. Presuming radiative decay occurs from the S_1 excited state, intersystem crossing (ISC) to T_1 states could also contribute to non-radiative decay. Indeed, calculated spin-orbit coupling (SOC) matrix elements (SOCMEs) show small but non-vanishing coupling between low-lying singlet and triplet states (Tables S26-S33). Comparing the geometries of (^{CF3}**L2**)$_2$Zn and (^{tBu}**L3**)$_2$Zn in their excited states, (^{tBu}**L3**)$_2$Zn undergoes more significant distortions in its optimized S_1 geometry compared to the ground state than does (^{CF3}**L2**)$_2$Zn. In particular, the *N*-phenyl ring is twisted by 10° in the lowest-lying singlet excited state of (^{tBu}**L3**)$_2$Zn compared to in the ground-state; there is no change to the comparable torsion angle involving the *N*-pyrimidinyl ring of (^{CF3}**L2**)$_2$Zn (Figure S12). Thus, the observation that tempering N_{amido} character through resonance can boost emission intensity evidently results from greater rigidity in the excited state helping to reduce non-radiative decay.[25] Efforts to further leverage this finding in the discovery of novel luminescent materials are presently underway.

Table 1. Absorption and emission data for the zinc complexes and proligands in CH_2Cl_2 at 295 K, except where stated otherwise.

Compound	Absorption [a] λ_{max} / nm (ε / $M^{-1}cm^{-1}$)	Emission at 295 K				Emission at 77 K [c]	
		λ_{max} / nm	Stokes shift / nm (eV)	PLQY [b]	τ / ns [b]	λ_{max} / nm	τ / ns
(^{CF3}**L1**)$ZnCl_2$	252 (26700), 302 (9180), 334 (6330), 348 (7160), **380 (3230)**	512	132 (0.84)	0.64	13	480	12
(^{tBu}**L1**)$ZnCl_2$	252 (33100), 303 (15700), 337 (8250), 347 (9010), **383 (3520)**	530	147 (0.90)	0.41	13	490	14
(^{CF3}**L2**)$_2$Zn	275 (40600), 305 (39600), 351 (17500), 368 (18500), **436 (12600)**	595	159 (0.76)	0.26	8	510, 535	10
(^{tBu}**L3**)$_2$Zn	313 (22500), 357sh (8180), 392 (6680), **513 (2540)**	*(d)*	*(d)*	*(d)*	*(d)*	*(d)*	*(d)*
^{CF3}**L1**	253 (17500), 293 (8320), 337 (4350), **370sh (2830)**	519	149 (0.96)	0.12	6	452	9
^{tBu}**L1**	291sh (12400), 330 (6750), **377sh (2060)**	528	151 (0.94)	0.06	11	467	13
^{CF3}**L2**	257 (58200), 298 (23500), 325 (20300), 337 (21700), 368 (7860), **393sh (2800)**	442	49 (0.35)	0.0013	*(e)*	392, 417, 439	8
^{tBu}**L3**	246 (21400), 270 (13700), 353 (4470), **393 (2730)**	502	109 (0.68)	0.0007	6	445, 464	7

(a) The lowest-energy band is shown in bold font. *(b)* Values in deoxygenated solution; the corresponding values in air-equilibrated solution were within the uncertainty on the measurements. *(c)* In diethyl ether / isopentane / ethanol (2:2:1 v/v). *(d)* No reliably detectable emission. *(e)* The lifetime of this complex was too short and / or the emission too weak to obtain a reliable lifetime.

Conflicts of interest

There are no conflicts to declare.

Notes and references

1 B. M. Hockin, C. Li, N. Robertson and E. Zysman-Colman, *Catal. Sci. Technol.*, 2019, **9**, 889–915.
2 T. E. Graedel, E. M. Harper, N. T. Nassar, P. Nuss and B. K. Reck, *Proc. Nat. Acad. Sci.*, 2015, **112**, 4257–4262.
3 A. Barbieri, G. Accorsi and N. Armaroli, *Chem. Commun.*, 2008, 2185–2193.
4 M. D. Allendorf, C. A. Bauer, R. K. Bhakta and R. J. T. Houk, *Chem. Soc. Rev.*, 2009, **38**, 1330–1352.
5 S. Bestgen, C. Schoo, B. L. Neumeier, T. J. Feuerstein, C. Zovko, R. Köppe, C. Feldmann and P. W. Roesky, *Angew. Chem., Int. Ed.*, 2018, **57**, 14265–14269.
6 K. Singh, I. Siddiqui, V. Sridharan, R. A. Kumar Yadav, J.-H. Jou and D. Adhikari, *Inorg. Chem.*, 2021, **60**, 19128–19135.
7 Y. Sakai, Y. Sagara, H. Nomura, N. Nakamura, Y. Suzuki, H. Miyazaki and C. Adachi, *Chem. Commun.*, 2015, **51**, 3181–3184.
8 N. Lüdtke, J. Kuhnt, T. Heil, A. Steffen and C. M. Marian, *ChemPhotoChem*, 2023, **7**, e202200142.
9 C. Trinh, K. Kirlkovali, S. Das, M. Ener, H. Gray, P. Djurovich, S. Bradforth and M. Thompson, *J. Phys. Chem. C*, 2014, 21834–21845.
10 V. Giuso, E. Jouaiti, C. Cebrián, S. Parant-Aury, N. Kyritsakas, C. Gourlaouen and M. Mauro, *ChemPhotoChem*, 2023, **7**, e202300092.
11 C. Bizzarri, E. Spuling, D. M. Knoll, D. Volz and S. Bräse, *Coord. Chem. Rev.*, 2018, **373**, 49–82.
12 T. S. Teets, D. V. Partyka, J. B. Updegraff and T. G. Gray, *Inorg. Chem.*, 2008, **47**, 2338–2346.
13 A. Gorman, J. Killoran, C. O'Shea, T. Kenna, W. M. Gallagher and D. F. O'Shea, *J. Am. Chem. Soc.*, 2004, **126**, 10619–10631.
14 T. S. Teets, D. V. Partyka, A. J. Esswein, J. B. Updegraff, M. Zeller, A. D. Hunter and T. G. Gray, *Inorg. Chem.*, 2007, **46**, 6218–6220.
15 S. Wang, *Coord. Chem. Rev.*, 2001, **215**, 79–98.
16 T. Sano, Y. Nishio, Y. Hamada, H. Takahashi, T. Usuki and K. Shibata, *J. Mater. Chem.*, 2000, **10**, 157–161.
17 I. B. Lozada, J. D. Braun, J. A. G. Williams and D. E. Herbert, *Inorg. Chem.*, 2022, **61**, 17568–17578.
18 D. E. Herbert, *Can. J. Chem.*, 2023, **101**, 892–902.
19 I. B. Lozada, T. Murray and D. E. Herbert, *Polyhedron*, 2019, **161**, 261–267.
20 J. D. Braun, I. B. Lozada, C. Kolodziej, C. Burda, K. M. E. Newman, J. van Lierop, R. L. Davis and D. E. Herbert, *Nat. Chem.*, 2019, **11**, 1144–1150.
21 P. Mandapati, J. D. Braun, I. B. Lozada, J. A. G. Williams and D. E. Herbert, *Inorg. Chem.*, 2020, **59**, 12504–12517.
22 I. B. Lozada, J. D. Braun, J. A. G. Williams and D. E. Herbert, *Inorg. Chem.*, 2022, **61**, 17568–17578.
23 A. V. Marenich, C. J. Cramer and D. G. Truhlar, *J. Phys. Chem. B*, 2009, **113**, 6378.
24 M. Kellogg, A. Akil, D. S. Muthiah Ravinson, L. Estergreen, S. E. Bradforth and M. E. Thompson, *Faraday Discuss.*, 2019, **216**, 379–394.
25 P. Mandapati, J. D. Braun, C. Killeen, R. L. Davis, J. A. G. Williams and D. E. Herbert, *Inorg. Chem.*, 2019, **58**, 14808–14817.